Real time control of air feed system in a PEM fuel cell by means of an adaptive neural-network

Victor M. Sanchez[1,*], Juan M. Ramirez[2], L.G. Arriaga[3], R. Barbosa[1]

[1]Depto. Ingeniería, Universidad de Quintana Roo,
Blvd. Bahía s/n E. I. Comonfort, 77019, Chetumal, Q. Roo, México.
[*]Tel: 98350300, vsanchez@uqroo.mx
[2]CINVESTAV – Unidad Guadalajara, Av. Científica 1145,
Col, El Bajío, Zapopan, Jal., México
[3]Centro de Investigación y Desarrollo Tecnológico en Electroquímica,
Pedro Escobedo, Querétaro, 76703, México

ABSTRACT

Fuel Cells (FCs) are electrochemical devices which convert chemical energy into electrical and thermal energy. Polymer Electrolyte Membrane (PEM) FCs are one of the most technology researched due to its high power density, solid electrolyte and low corrosion. Moreover, these FCs operate at low temperatures (50 ºC – 100 ºC) which allow fast start-up. However, their use and research is limited due to their high costs, the complex control task required and the lack of proper electronic converter for the power conditioning produced by the FCs. In steady state, the generating process of the PEMFC is generally fast and depends on the replacing speed of the gases consumed in order to meet the demanded energy. However, when an important power transient arises an oxygen starvation may happen in the FC, due to the slow transient response of the mechanical devices used for the hydrogen and oxygen supply. The adequate replenishment of the depleted oxygen avoids the oxygen starvation phenomenon and extends the FC's life time. This paper proposes an adaptive B-spline neurocontroller (B-SNN) for the optimal oxygen supply into the PEMFC. The B-SNN is proposed due to its simple structure, adaptability, and robustness, taking into account the PEMFC's nonlinearities. Furthermore, B-SNN has the capabilities of on-line learning and real time operation. The proposed neurocontroller is tested on a PEMFC hardware-in-loop emulator. The FC emulator is based on a detailed nonlinear simulator taken from the open literature. Real time results of the PEMFC system emulator and the neurocontroller obtained by the hardware-in-the-loop strategy are exhibited.

1. Introduction

The PEMFCs have become popular as alternative power source due to its environmental and high efficiency properties. These qualities make of the PEMFCs the best option in applications of transport and mid-sized distributed generators in which fast dynamic responses over time are required. Even with the advantages of the PEMFCs as portable power sources, their use is limited due to their high costs and complex control task required.

PEMFC uses hydrogen and oxygen in order to generate energy. The hydrogen is get from a storage medium of hydrogen, usually pressurized tanks. This fact does more easily the hydrogen supply to the PEMFC due that hydrogen flow is controlled through some valves.

Oxygen supply is different due to it is taken from the environment and it is introduced to the PEMFC through a compressor driven by an electric motor. However, the oxygen amount in the air varies with the geographic location where the PEMFC application is implemented. During a power transient, the PEMFC consumes hydrogen and oxygen, but if the depletion of these reagents is important, a starvation condition could occur and the PEMFC could suffer an irreversible damage. Oxygen supply during a power transient becomes the main control problem for the PEMFC system due to the slow transient response of the mechanical devices used for its supply.

For this reasons, the oxygen supply is a critical point in the FC's safety. The oxygen supply is made through a compressor, driven by an electrical motor, which regulates the air supply. The motor may be fed from the FC. Thus, during its starting, the PEMFC requires a rapid increment of air supply, in order to avoid the oxygen starvation condition. Thus, the PEMFC's air management plays an important role in the overall performance since it absorbs around 25% of the fuel cell energy [1]. Likewise, this fact is a great challenge to obtain an efficient control for the air management system, due to the nonlinear interactions among the different FC's auxiliary systems.

The interaction among the auxiliary systems and the PEMFC stack originates several unknown parameters that should be considered in the controller's design for an optimal and safety operation condition of the PEMFC system.

The use of artificial neural networks (ANNs) offers an attractive alternative for controlling the oxygen supply. ANNs are able to model and control on-line nonlinear and non-stationary systems. A neuro-controller considers the practical systems complexity, and provides a realistic control model, with less computation time over a wide range of operating conditions [5].

There are several references to the PEMFC system control based on ANNs [2-5]. However, the ANNs algorithms used in these works are trained off-line, or based in a linear model of the PEMFC. In this paper a B-Spline Neural Network (B-SNN) is employed for the oxygen supply control. B-SNN is able to learn on-line the nonlinear PEMFC dynamic. Hardware-in-loop results obtained from a PEMFC system emulator driving linear and nonlinear loads are shown.

This paper is organized as follows. Section 2 presents the fuel cell model, the B-spline neural network and the control strategy. Section 3 discusses results obtained by a hardware-in-the-loop emulation. Finally, section 4 summarizes some conclusions.

2. Design of the B-spline neuro-controller.

2.1 Fuel Cell system model

Different auxiliary components are required for the PEMFC operation. These components provide the reactant gases, regulate the temperature and humidity, and guarantee the PEMFC safety. Figure 1 depicts the schematic diagram of a fuel cell system, which includes one stack and three subsystems: (i) hydrogen supply, (ii) air supply with humidification, and (iii) thermal management system.

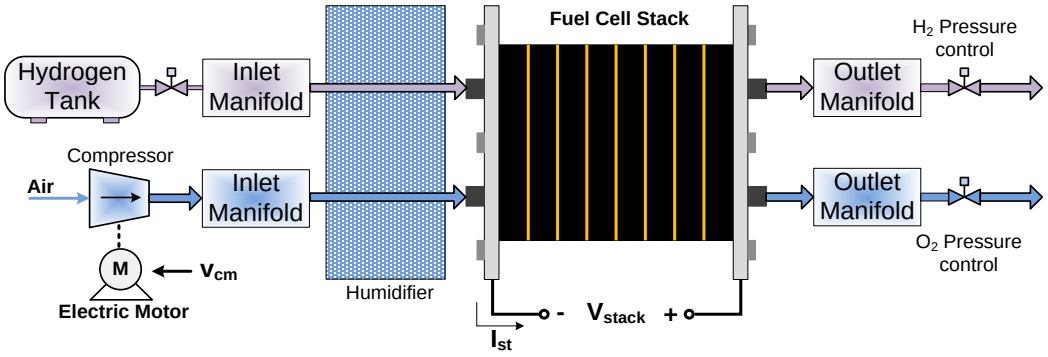

Figure 1. PEM Fuel Cell system model.

The auxiliary components presented in the Figure 1 may be merged in two sub-systems: (i) air feed system, which provides oxygen and humidity to the cathode; and (ii) the hydrogen supply system for the anode. The first one is constituted by an electric motor, an air compressor, the air cooler, and the humidifier. The mathematical models of the auxiliary systems and PEMFC stack are taken from the detailed model presented in [6]. This PEMFC system model was selected due to that includes the behavior of the PEMFC stack model as well as its auxiliary systems. The corresponding mathematical model has been exposed and validated in [7-9].

The assumptions for the stack's modeling are: (i) gases obey the ideal gas law; (ii) the temperature of the flow inside the cathode flow channel is equal to the stack temperature (80ºC); (iii) there is a constancy in the gases' volume (input-through-output). The proper performance of the auxiliary systems contributes to the FC's efficient operation. Among these systems, the air feed system is used to control the power generated by the FC system.

2.1.1 Air feed system

The air feed system consists of a compressor driven by an electrical motor, so that the compressor's output can be controlled by the voltage fed to the motor.

The air mass flow rate produced by the compressor, W_{cr}, is a function of the ratio between the atmospheric pressure, the inlet manifold pressure, and the compressor's speed. Thus, the corresponding nonlinear flow's characteristic is approximated by a map data, where a linear function is obtained through curve fitting techniques proposed by Jensen-Kristensen [10]. The method consists in determining the normalized compressor flow rate through a least square fit on experimental data, by the following relationship:

$$\varphi = \frac{k_3\Psi - k_1}{k_2 + \Psi} \quad (1)$$

where φ is the normalized compressor flow rate, *k1*, *k2*, *k3* are coefficients determined through least square fit and Ψ is the dimensionless head parameter. Based on (1) the air mass flow of the compressor (W_{cr}) is calculated using:

$$W_{cr} = \phi p_a \frac{\pi}{4} d_c^2 U_c \quad (2)$$

where d_c is the compressor diameter, p_a is the air density and U_c is the compressor blade tip speed. Likewise, the electro-mechanical equation is taken into account,

$$J_{cp}\dot{\omega}_{cp} = \tau_{cm} - \tau_{cp} \quad (3)$$

where J_{cp} is the compressor inertia, ω_{cp} is the compressor angular speed, τ_{cm} and τ_{cp} are the compressor motor torque and compressor load torque, respectively. The air flow of the compressor is controlled by the motor voltage, which is a function of the current drawn from the stack. The compressor motor torque is calculated as a function of the motor's voltage v_{cm} (4).

$$\tau_{cm} = \eta_{cm} \frac{k_t}{R_{cm}} \left(v_{cm} - k_v \omega_{cp}\right) \quad (4)$$

where k_t, R_{cm} and k_v are motor's constants and η_{cm} is its mechanical efficiency. The control objective in the cathode is to control the oxygen supply through the motor voltage control. Oxygen excess ratio, λ_{O2}, is a FC performance parameter to evaluate the oxygen supply and it is described by (5).

$$\lambda_{O_2} = \frac{W_{O_{2,in}}}{W_{O_2,react}} \quad (5)$$

where $W_{O2,in}$ is the oxygen mass flow rate entering to the cathode, and $W_{O2,react}$ is the rate of reacted oxygen.

2.2 B-spline neurocontroller design

The ANN-based controllers major advantages are their design simplicity, and their tradeoff between complexity and performance. The B-SNN is a particular case of neural networks that are able to adaptively control a system, with the option of carrying out such tasks on-line, taking into account the non-linearities [11-13]. Additionally, through B-SNN there is a possibility to limit the input space by the basis functions definition. The most important feature of the B-spline strategy is its output smoothness that is due to the basis functions. Their size, shape, and overlap determine how the network generalizes into the *m*-dimensional input space. Some parameters have to be specified, such as the basis functions and the learning rate. The B-SNN can adaptively be updated to follow changes of the system operation state and to compensate external disturbances. This is due to the weighting vector, which is updated on-line within each data sampling.

In this paper, the oxygen excess ratio must attain a reference value through the B-spline adaptive control. That is, the neurocontroller must drive the compressor voltage, v_{cm}, to the desired value in order to regulate the fed oxygen to the PEMFC cathode. The B-spline neural network output is [14],

$$y = \sum_{i=1}^{p} a_i w_i \qquad (6)$$

where w_i and a_i are the i^{th} weight and the i^{th} B-spline basis function output, respectively; p is the number of weights. Let us define

$$\mathbf{w} = [w_1\ w_2 \ldots w_p]^T, \qquad \mathbf{a} = [a_1\ a_2 \ldots a_p]^T$$

Thereby, eqn. (6) can be rewritten as

$$y = \mathbf{a}^T \mathbf{w} \qquad (7)$$

The input space is normalized by a lattice on which the basis functions are defined. The transformed input vector, **a**, is generally sparse, which means that the knowledge is stored and adapted locally. That is, only a fixed number of basis functions participate in the network output. Therefore, the weights are not necessarily calculated each time step, thus reducing the computational effort and time execution, making the B-spline NN suitable for on-line adaptive control. The basis functions are defined by the following recurrent relationship:

$$N_k^j(x) = \left(\frac{x-\lambda_{j-k}}{\lambda_{j-1}-\lambda_{j-k}}\right)N_{k-1}^{j-1}(x) + \left(\frac{\lambda_j - x}{\lambda_j - \lambda_{j-k+1}}\right)N_{k-1}^{j}(x) \quad (8)$$

$$N_1^j(x) = \begin{cases} 1 & if\ x \in I_j \\ 0 & otherwise \end{cases} \quad (9)$$

where λ_j is the j^{th} knot and I_j (=[λ_{j-1}, λ_j]) is the j^{th} interval. In this paper, the B-SNN neurocontroller is constituted by four-univariate order-two basis functions, Figure 2.

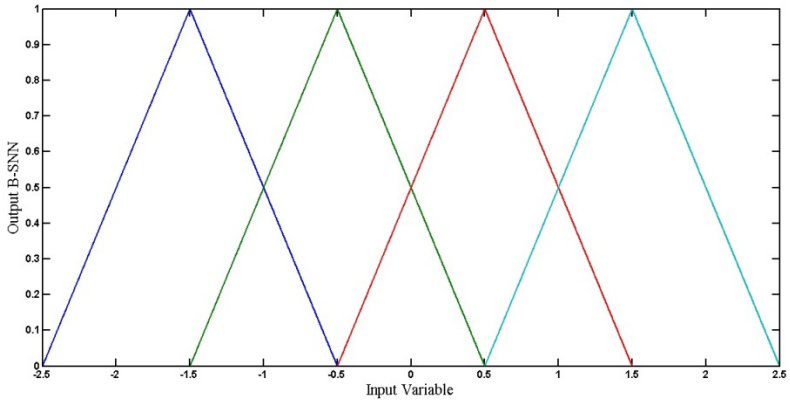

Figure 2. B-spline basis functions of order-two.

The neurocontroller's output is the compressor voltage, v_{cm}, which compensate the error between the reference oxygen excess ratio and the measured value (e_y), Figure 3.

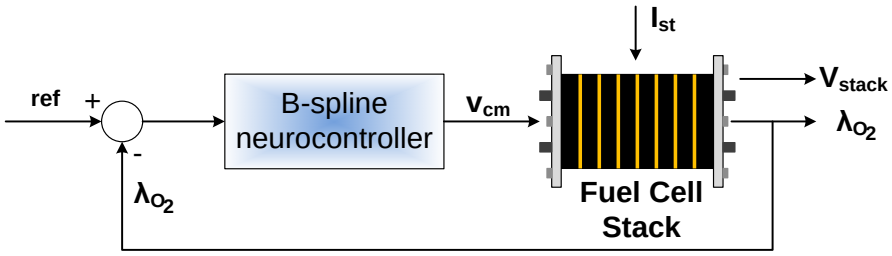

Figure 3. B-SNN control scheme.

In this paper, the basis functions are evaluated as a function of the oxygen excess ratio error, and were bounded within [-2.5, 2.5], Figure 2. The control objective is to maintain λ_{O2} = 2, because this value prevents oxygen starvation condition and it is close to a high efficiency range [8]. The neural controller's weights are estimated on-

line using the following instantaneous learning rule [15],

$$w_i(t) = w_i(t-1) + \frac{\eta\, e_i(t)}{\|\mathbf{a}(t)\|_2^2} a_i(t) \qquad (10)$$

where: η is the learning rate and is the instantaneous output error.

The learning rate has to be elected for obtaining a smooth response and its value can be: $0 < \eta < 2$, [14]. Weights converge, if and only if, the learning rate satisfies the previous condition. The learning rate is adjusted by trial-and-error, in this application it is tuned in 1.8. Hence, the B-SNN training process is carried out continuously on-line, while the weights' values are updated using the feedback variable. The neural network output is calculated by (7).

PEMFC model system and the air management control are implemented on a dSPACE® platform. A dSPACE1104 board is utilized. Due to the complexity of the whole system a sampling frequency of 500 Hz is used to the hardware-in-the-loop evaluation. Sampling frequency is less than the constant time of the auxiliary subsystems so that it does not affect the behavior of the PEMFC system. Figure 4 displays the comparison between simulation obtained by Simulink and the results of the dSPACE® platform for the stack voltage.

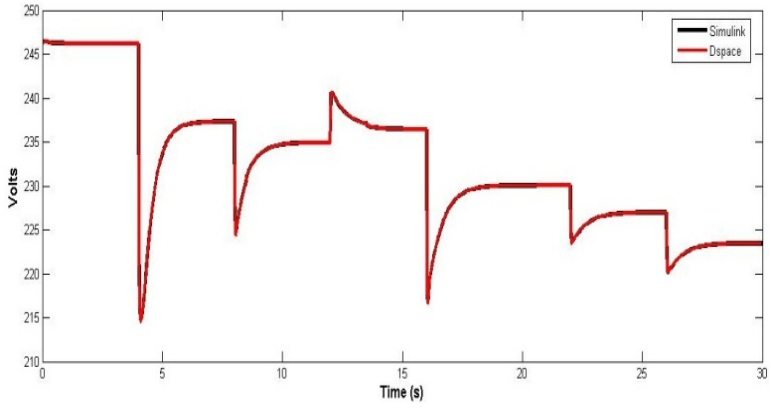

Figure 4. Comparison between Simulink® and the dSPACE® platform for the stack voltage

3. Results and discussions.

In order to illustrate the B-SNN performance, a comparison with a static feed-forward and Proportional-Integral (PI) feedback controllers is carried out. The results presented in this section have been calculated form hardware-in-loop setup based on dSPACE® platform. A series of load-current steps, ranging from 100 A to 300 A, have been tested in

order to evaluate the performance of the three controllers: Feed-forward, PI, and B-SNN. Figure 9 shows the current profile applied to the PEMFC system.

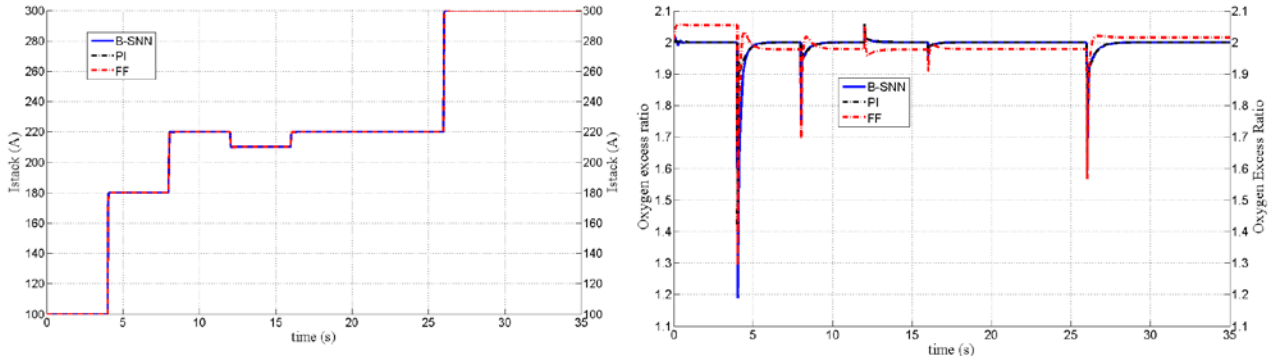

(a) (b)

Figure 9. Comparison of the B-SNN controller with feed-forward and PI controllers. (a) Load current profile. (b) PEMFC system response with feed-forward, PI and B-SNN controllers.

The B-SNN and PI controllers exhibit a better performance that the one achieved with the feed-forward controller because this latter presents and offset in steady-state. Feed-forward offset makes that the compressor motor consumes power in excess, which decreases the net PEMFC's power. Also, the feed-forward offset leads to higher consumption of hydrogen and oxygen. In addition, the feed-forward controller's overshoots are disadvantageous because bigger power is required from the compressor. On the other hand, the B-SNN and PI controllers can maintain the oxygen excess ratio within the desired value; however, the B-SNN controller shows the biggest overshoot in the first current-step. In order to notice the controllers' transient response, Figure 10 shows a zoom at = 4 s, when one 80 A current-step happens.

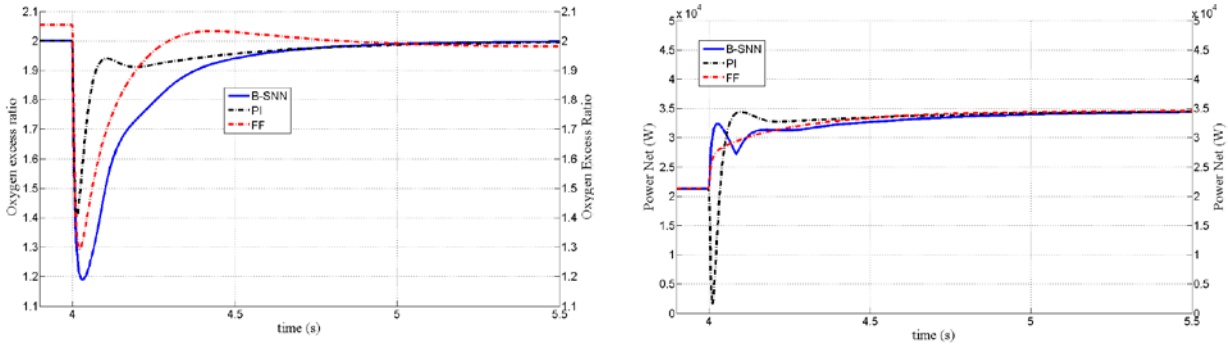

(a) (b)

Figure 10. Detail of step load current in t = 4s. (a) Oxygen excess ratio. (b) Power net of the PEMFC system during the transient.

According to Figure 10(a), the PI response shows a better performance than that of the B-SNN and feed-forward controllers because of it exhibits less overshoot and fastest response. However, this PI response produces an important decrease of the PEMFC net power due to an over-demand of the compressor, as it is detailed in Figure 10(b). During the transient, the compressor requires additional power, which is taken from the PEMFC system. The PI controller commands the compressor to respond quickly in order to replenish the oxygen depleted during the transient; however, the compressor consumes an important power amount that almost consumes all the energy generated by the PEMFC stack. This power drop can compromise the global performance of the PEMFC system. On the other hand, the B-SNN controller exhibits a soft response that avoids that the PEMFC system falls in a starvation condition ($\lambda_{O_2} < 1$), at the same time that avoids an excess power consumption of the compressor.

Detail of the compressor's power in t = 4s is shown in Figure 11(a), where the power-overshoot produced by the PI controller during the current transient of 80 A is noticed. Figure 11(b) shows the voltages provided by the controllers to the compressor motor, where the biggest voltage-overshoots during transients are produced by the PI controller

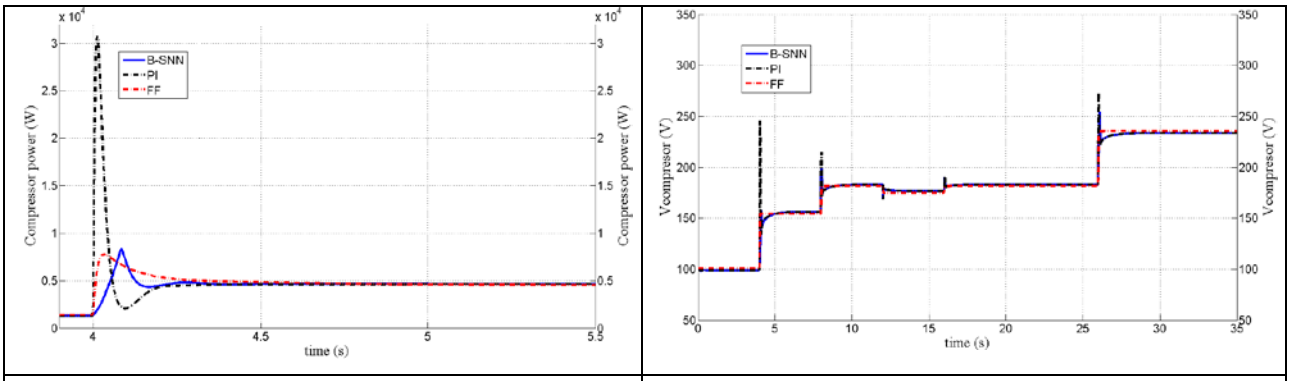

(a) (b)

Figure 11. (a) Zoom of the compressor power in t = 4 s. (b) Compressor motor voltage

These results demonstrate that the B-spline neural network controller may be an interesting choice to regulate the PEMFC. The main advantages of this neuro-controller are the on-line learning and its adaptive control, without a previous training.

4. Conclusions

In this work, B-SNN neurocontroller is synthesized and assembled in order to supply an adequate oxygen flow to the PEMFC stack. By the proposed neural control the possibility to implement the on-line control is potential due to it has learning ability and adaptability, as well as robustness, simple control algorithm and rapid calculations. These are desirable characteristics for practical hardware implementation on the power systems environments.

The B-spline NN control exhibits adaptive behavior since the weights can be adapted on-line responding to inputs and error values as they take place. Also, it may take into account non-linearities, non-modeled dynamics, and non-measurable noise. Hardware-in-loop results under load current steps demonstrate the effectiveness and robustness of the neurocontroller. Likewise, they show the appropriate performance of the controller, while rapid reference tracking is achieved as well as a satisfactory transient response is attained.

5. Acknowledgments

The authors wish to thank to PROMEP for the support for this project under grant UQROO-EXB-072

6. References

[1] S. Pischinger, C. Schonfelder, O. Lang, “Development of fuel cell system air management utilizing HIL tools,” *in Proc. Fuel Cell Power Transp.*, 2002, pp. 109-117.

[2] Marsala G., Bouquin D., Pukrushpan J., Pucci M., Cirrincione G, Vitale G, et. al., “A neural inverse control of a PEM-FC system by the generalized mapping regressor (GMR)”, *IEEE industry application annual meeting*, 2008, pp. 1-12.

[3] Hatti M., Tioursi M., “Dynamic neural network controller model of PEM fuel cell system,” *International Journal of Hydrogen Energy* 2009 (34), pp. 5015-21.

[4] Bao C., Ouyang M. Yi B.,“Modelling and control of air steam and hydrogen flow with recirculation in a PEM Fuel Cell system-II Linear and adaptive nonlinear control,” *International Journal of Hydrogen* 2006 (31), pp. 1897-913.

[5] Chen Q., Quan S. and Xie C., “Nonlinear predictive control for oxygen supply of a fuel cell system,” *in Proc. of International Joint Conference on Neural Networks* 2009, pp. 518 - 521.

[6] Pukrushpan J., Stefanopoulou A. and Peng H., "Modelling and control for pem fuel cell stack system," *Proc. of the American Control Conference* 2002, vol. 4, pp. 3117-3122.

[7] Pukrushpan J., Stefanopoulou A. and Varigonda S., "Control oriented model of fuel processor for hydrogen generation in fuel cell applications,"*IFAC Symposium in Advances in Automotive Systems* 2004.

[8] Pukrushpan J., Stefanopoulou A. and Peng H., "Control of Fuel Cell Power Systems," *Springer Verlag London*, 2005.

[9] Gelfi S, Stefanopoulou A. Pukrushpan J and Peng H, "Dynamics of low pressure and high pressure fuel cell air supply systems," *Proc. of the American Control Conference* 2003, vol. 3 pp. 2049-2053.

[10] Moraal P. and Kolmanovsky I,, "Turbocharger modeling for automotive control applications," *SAE paper* 1990-01-0908.

[11] Shuang Cong, and Ruixiang Song, "An Improved B-Spline Fuzzy-Neural Network Controller", *Proc. 3rd World Congress on Intelligent Control and Automation* 2000, pp. 1713-1717.

[12] K. W. E. Cheng, H. Y. Wang, and D. Sutanto, "Adaptive directive neural network control for three-phase AC/DC PWM converter", *IEE Proc. Electr. Power Appl.* 2001, vol. 148, pp. 425-430.

[13] D.S. Reay, "CMAC and B-spline Neural Networks Applied to Switched Reluctance Motor Torque Estimation and Control", *IEEE Industrial Electronics Society 29th Annual Conf.* 2003, pp. 323-328.

[14] Brown, and C. Harris, Neurofuzzy Adaptive Modelling and Control, *Prentice Hall International*, 1994.

[15] David Saad, “On-line learning in neural networks,” *Cambridge University Press* 1998.